We are IntechOpen,
the world's leading publisher of
Open Access books
Built by scientists, for scientists

6,900
Open access books available

185,000
International authors and editors

200M
Downloads

154
Countries delivered to

Our authors are among the

TOP 1%
most cited scientists

12.2%
Contributors from top 500 universities

WEB OF SCIENCE™

Selection of our books indexed in the Book Citation Index
in Web of Science™ Core Collection (BKCI)

Interested in publishing with us?
Contact book.department@intechopen.com

Numbers displayed above are based on latest data collected.
For more information visit www.intechopen.com

Photonic Quasicrystals for Filtering Application

Youssef Trabelsi

Abstract

In this chapter, we study the properties of specific one dimensional photonic quasicrystal (PQCs), in order to design an output multichannel filter. We calculate the transmittance spectrum which exhibits a photonic band gap (PBG), based on the Transfer Matrix Method (TMM) and the two-fluid model. We show that the generalized Thue-Morse (GTM) and generalized Fibonacci GF(m, n) distributions provide a stacking of similar output multichannel with zero transmission when the input was a sharp resonance of peaks at given $n = 2pm$ where p, is a positive integer. Also, we consider GTM configuration and we apply a deformation $y = x^{h+1}$ along the PQC filter, which enhanced the band width of each channel with respect to the number of peaks inside the main transmittance. Here, the coefficient h represents the deformation degree, x and y are thicknesses of the layers before and after the deformation, respectively. This improves the characteristics of PBG.

Keywords: hybrid quasiperiodic PC, superconducting materials, GTM sequence, GF sequence, multichannel optical filters, deformed 1D photonic quasicrystals

1. Introduction

Photonic quasicrystals (PQCs) which are made of alternating dielectric and superconductor layers intervene in numerous researches due to their interesting optical properties [1–5]. This type of crystal is an artificial super lattice which is built according to quasiperiodic sequences. It is considerably different than photonic crystals (PCs) since it is a non-periodic structure with perfect long-range order and lack translational and it can be considered as an intermediate class between the random and periodic media. Our considered PQC consists of a stack of two different layers A and B which represent building blocks having a self-similarity distribution and long range order with no translational symmetry.

We mention that there are numerous examples of aperiodic chains constructed by a substitution rule. These chains allow forming many deterministic PQCs structures such as: Fibonacci, Thue-Morse, Rudin-Shapiro, Cantor, and Doubly periodic sequences.

Based on PQC heterostructure, many studies have been performed to carry out new optical devices. In this direction, the introduction of superconducting materials into the regular PQC photonic structure has been investigated in [5–7] in order to improve the characteristics of photonic band gap structures (PBGs) by changing the operating temperature of superconducting layers.

Recently, 1D deterministic multilayered structure including superconducting layers have attracted much attention in developing new kinds of optical filters which make new PQCs devices for optoelectronic system [5, 8–11]. These quasiperiodic filters have been extended to thermally photonic crystals, including certain cascades superconducting/dielectric layers. It may be used in specific operations as specifying thermal sensors for remote sensing applications. In [12], the authors used superconductors instead of metals within the PC because of the damping of electromagnetic waves in metals. Moreover, the properties of PC including superconductors are mainly depending on the temperature T. In this chapter, based on hybrid dielectric/superconductor photonic quasicrystals, we develop a multichannel optical filter with tenability around two telecom wavelengths. The main multilayered stacks are organized following quasiperiodic sequences. Hence, a multitude of channel frequencies with zero transmission can be created inside the main photonic band gap (PBG), which offers a resonance state due to the specific defects insert along the structures.

The characteristics of PBGs depend on the parameters of sequences, the thickness of the superconductor and the operating temperature. Furthermore, a multitude of transmission peaks were created within the main PBG which shifted with temperature of superconductors and lattice parameters of the aperiodic sequence.

We also show that, by monitoring the parameters of GTM, the transmission spectrum exhibit at limited gaps a cutoff frequency which is sensitive to the temperature of superconducting layers. The properties of stop channel frequencies can be notably enhanced by applying a whole deformation $y = x^{h+1}$. Here, x is the main PQC and y the structure after deformation. It is found that the gaps broad in with the increase of h. Thus, the main structure can be used to design a useful tunable multichannel filter in the optical information field.

2. Problem formulation

In all this work, the photometric response (transmission and reflection) through the 1D photonic quasicrystal which contains superconductors, are determined by using the Transfer Matrix Method (TMM). We use also the theoretical Gorter-Casimir two-fluid model [13, 14] to describe the properties of the superconductor material (YBa$_2$Cu$_3$O$_7$).

The application of the two-fluid models and Maxwell's equations through, imply that the superconducting materials' electric field equation, obeys to the following equation:

$$\nabla^2 E + k_s^2 E = 0 \tag{1}$$

Where the wave number satisfies the corresponding equality:

$$k_s = \sqrt{\frac{\omega^2}{c^2} - \frac{1}{\lambda_L^2}} \tag{2}$$

with μ_0 and $c = 1/\sqrt{\mu_0 \varepsilon_0}$ denote the permeability and the speed of light in free space, respectively.

As mentioned above, the electromagnetic response of superconducting materials with the absence of an external magnetic field was defined by the Gorter-Casimir two-fluid models (GCTFM) in [13, 14]. According to GCTFM, the complex conductivity of a superconductor satisfies the following expression:

$$\sigma(\omega) = \frac{-ie^2 n_s}{m\omega} \tag{3}$$

Where n_s is the electron density and ω is the frequency of incident electromagnetic wave. Moreover, e and m represent the charge and the mass of electron, respectively. Under the approximation condition indicated in [14], the imaginary part of conductivity is given as follows:

$$\sigma(w) \approx \frac{-i}{\omega\mu_0\lambda_L^2(T)} \tag{4}$$

where λ_L signifies the term of London penetration depths and satisfies the following equality:

$$\lambda_L^2 = \frac{m}{\mu_0 n_s e^2}. \tag{5}$$

The complex conductivity is given by this formula: $\sigma = \sigma_1 - j\sigma_2$, where σ_1 and σ_2 are the real and imaginary parts of σ. Thus, the complex conductivity satisfies [14]:

$$\sigma_2 = \frac{1}{\omega\mu_0\lambda_L^2(T)}, \tag{6}$$

where ω is the operating frequency. The London temperature-dependent penetration depth is:

$$\lambda_L(T) = \frac{\lambda(0)}{\sqrt{1 - G(T)}} \tag{7}$$

Where $\lambda(0)$ denotes the London temperature penetration depth at T = 0 K, and G(T) is the Gorter-Casimir function. In this case, $G(T) = (T/T_c)^2$, where T_c and T are the critical and the operating temperatures of the superconductor, respectively.

Based on the Gorter-Casimir theory, we obtain that the relative permittivity of lossless superconductors takes the following equality [14]:

$$\varepsilon_s = 1 - \frac{\omega_{th}^2}{\omega^2}, \tag{8}$$

where ω_{th} is the threshold frequency of the bulk superconductor which satisfies: $\omega_{th}^2 =\sim c^2/\lambda^2$.

Then, the refractive index of the superconductor is written as follows:

$$n_s = \sqrt{\varepsilon_s} = \sqrt{1 - \frac{1}{\omega^2\mu_0\varepsilon_0\lambda_L^2}}, \tag{9}$$

In the following, the photometric response through the 1D photonic quasicrystal which contains superconductors, is extracted using the Transfer Matrix Method (TMM). This approach shows that the determination of the reflectance R and the transmittance T depends on refractive indices n_s and lower refractive indices n_d.

According to TMM, the transfer matrix C_j verifies the following expression [15]:

$$\begin{bmatrix} E_0^+ \\ E_0^- \end{bmatrix} = \prod_{i=1}^{m} \frac{C_j}{t_j} \begin{bmatrix} E_{m+1}^+ \\ E_{m+1}^- \end{bmatrix}, \tag{10}$$

For both TM and TE modes, C_j satisfies:

$$C_j = \begin{pmatrix} \exp\left(i\varphi_{j-1}\right) & r_j \exp\left(-i\varphi_{j-1}\right) \\ r_j \exp\left(i\varphi_{j-1}\right) & \exp\left(-i\varphi_{j-1}\right) \end{pmatrix}, \tag{11}$$

Where φ_{j-1} denotes the phase between the two succeed interfaces and it is given by the following formula

$$\varphi_{j-1} = \frac{2\pi}{\lambda} \hat{n}_{j-1} d_{j-1} \cos\theta_{j-1} \tag{12}$$

For the two polarizations (p) and (s), the Fresnel coefficients t_j and r_j take the following equalities [15]:

$$r_{jp} = \frac{\hat{n}_{j-1}\cos\theta_j - \hat{n}_j\cos\theta_{j-1}}{\hat{n}_{j-1}\cos\theta_j + \hat{n}_j\cos\theta_{j-1}}; \quad t_{jp} = \frac{2\hat{n}_{j-1}\cos\theta_{j-1}}{\hat{n}_{j-1}\cos\theta_j + \hat{n}_j\cos\theta_{j-1}}$$

$$r_{js} = \frac{\hat{n}_{j-1}\cos\theta_{j-1} - \hat{n}_j\cos\theta_j}{\hat{n}_{j-1}\cos\theta_{j-1} + \hat{n}_j\cos\theta_j}; \quad t_{js} = \frac{2\hat{n}_{j-1}\cos\theta_{j-1}}{\hat{n}_{j-1}\cos\theta_{j-1} + \hat{n}_j\cos\theta_j}, \tag{13}$$

where $\hat{n}_j$ and θ_j are respectively the refractive indices and the angle of incidence in the jth layer which obey to the Snell's law: $\hat{n}_{j-1}\sin_{j-1} = \hat{n}_j\sin_j$ with $j\in[1, m+1]$.

Consequently, the transmittance satisfies [15]:

$$T_{rs} = \mathrm{Re}\left(\frac{\hat{n}_{m+1}\cos\theta_{m+1}}{\hat{n}_0\cos\theta_0}\right)|t_S|^2; \quad T_{rp} = \mathrm{Re}\left(\frac{\hat{n}_{m+1}\cos\theta_{m+1}}{\hat{n}_0\cos\theta_0}\right)|t_P|^2, \tag{14}$$

3. Generalized quasiperiodic sequences

3.1 Generalized Thue-Morse sequence

A one dimensional GTM sequence is called aperiodic because it is more disordered than the quasiperiodic one. In addition, the two different materials included in one dimensional GTM system should be structured by applying the substitution rule: $\sigma_{GTM}(H, L) : H \rightarrow H^m L^n, L \rightarrow L^m H^n$ [16], where H and L represent the two layers, having the higher and the lower refractive indices, respectively. We note that the Fourier spectra of the GTM sequence is singular and continuous. Also, the GTM quasiperiodic chain is generated by a recursive deterministic sequence S_{k+1} verifying: $S_{k+1} = S_k^m \overline{S}_k^n$, where $\overline{S}_k^n$ is the conjugated sequence of S_k^n, m and n are the parameters of GTM sequence with order k. This rule can be applied to two dimensions: horizontally and vertically.

Based on GTM sequence S_{k+1}, we give **Table 1** which illustrates an example of organized multilayered stacks (H, L) for m = n = 2.

The configuration of the proposed 1D photonic dielectric/quasiperiodic superconducting layers which is built according to the GTM sequence is shown in **Figure 1**.

3.2 Generalized Fibonacci sequence

1D Fibonacci quasiperiodic sequences are constructed by applying the inflation rule in [17]: $\sigma_{GF}(H, L) : H \rightarrow HL, L \rightarrow H$ for the two blocks H and L, where H

Order of GTM	Organized $\{H, L\}$ blocks according GTM(2, 2) sequence
1	HHLL, with S_0 = H
2	HHLLHHLLLLLHHLLHH
3	HHLLHHLLLLLHHLLHHHHLLHHLLLLLHHLLHH LLHHLLHHHHLLHHLLLLLHHLLHHHHLLHHLL

Table 1.
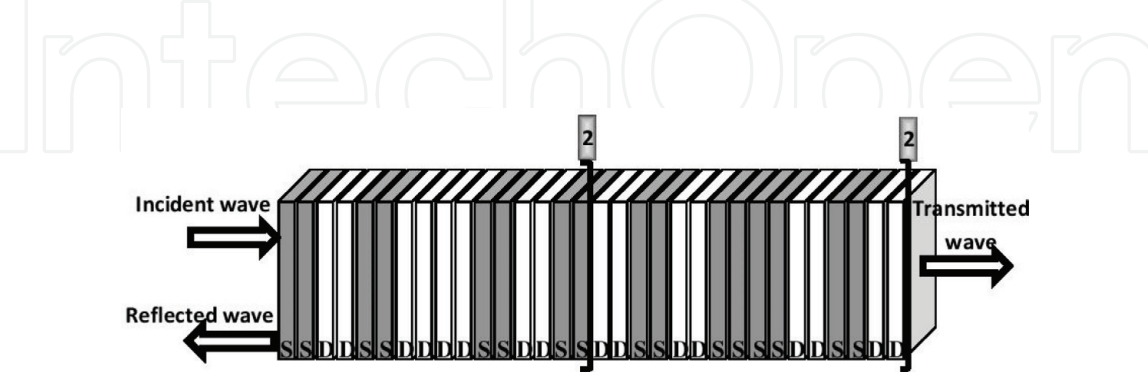*Repeated {H,L} blocks determined by applying the substitution rule $\sigma_{GTM}(H,L)$.*

Figure 1.
Schematic drawing of 1D multilayered stacks made of dielectric (D)/superconducting materials (S), built according to the GTM(2, 2) sequence.

denotes the material with the higher refractive index, and L denotes the material with the lower refractive index. The GF chain is generated using the substitution rule: $\sigma_{GF}(H, L) : H \rightarrow H^m L^n, L \rightarrow H$. Thus, the GF sequence S_{k+1} satisfies the recursion relation: $S_{k+1} = S_k^m S_{k-1}^n$ with k is the order of GF sequence.

The Fourier transform of Fibonacci class of quasicrystal gives discrete values which represent the significant property of crystals. We note that the eigenvalues of related matrix Fibonacci spectrum are Pisot numbers. For the Fibonacci-type, the material waves interfere constructively in appropriate length. The analysis of Fibonacci quasicrystals submitted to X-ray diffraction shows a multitude of Bragg peaks. Moreover, quasicrystals which are based on the Fibonacci distribution ordered at long distances, show a typical construction without a forbidden symmetry. Hence, the generalized Fibonacci (GF) type gives some basic proprieties which are identical to those given by simple Fibonacci class such as Fourier spectrum with Bragg peaks, inflation symmetry and localized critical modes with zero transmission called pseudo band gaps. In a generic form of the organized multilayers (H, L) through Fibonacci sequence, the four multilayered stacks are grouped in **Table 2**.

As an example, the third order of GF(m, n) quasiperiodic photonic structure containing alternate dielectric (D) and superconducting layers (S) with m = n = 2 is shown in **Figure 2**.

Order of GF	Organized $\{H, L\}$ chain according GF(2, 2) sequence
1	HHLL, with S_0 = L and S_1 = H
2	HHLLHHLLHH
3	$H^2 L^2 H^2 L^2 HHH^2 L^2 H^2 L^2 HHH^2 L^2 H^2 L^2$
4	$H^2 L^2 H^2 L^2 HHH^2 L^2 H^2 L^2 HHH^2 L^2 H^2 L^2 H^2 L^2$ $H^2 L^2 HHH^2 L^2 H^2 L^2 HHH^2 L^2 H^2 L^2 H^2 L^2 H^2 L^2 HH \, H^2 L^2 H^2 L^2 HH$

Table 2.
Generation of Fibonacci sequence and organized blocks (H, L) repeated by the substitution rule $\sigma_{GF}(H,L)$.
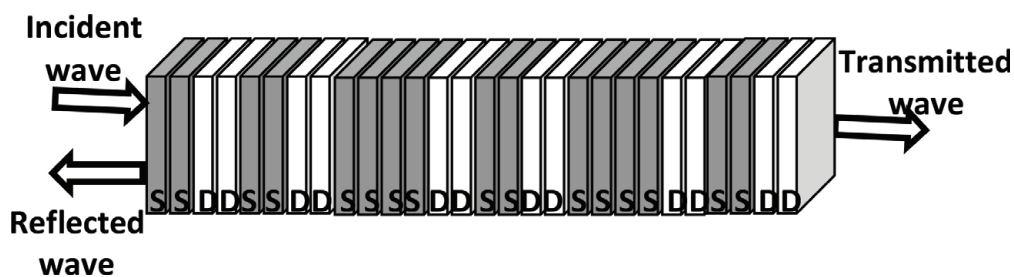
Figure 2.
Schematic representation showing the third generation of 1D GF(m, n) quasi-periodic multilayered stacks consisting of alternate dielectric (D)/superconducting materials (S).

4. Results and discussion

4.1 Multichannel filter narrow bands by using GTM sequence

4.1.1 Effect of GTM(m, n) parameters

In this subsection, we give the transmission properties of GTM and GF quasi-periodic one-dimensional photonic crystals (1DPCs) which contain
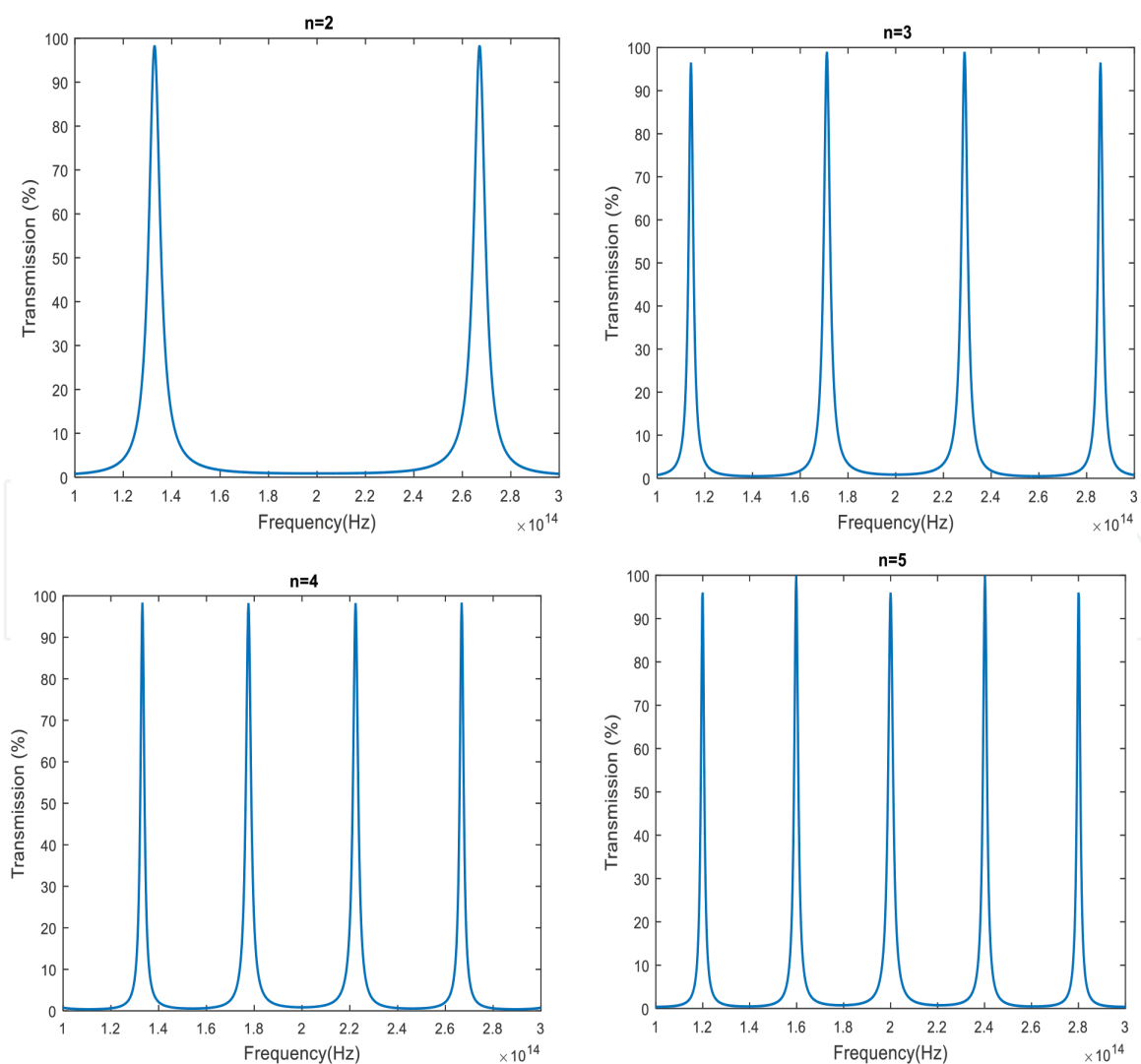

Figure 3.
Transmittance spectrum versus frequencies of hybrid GTM multilayered stack at given parameters: n is set at 2, 3, 4 and 5 for m = 2.

superconductors. We recall that our one dimensional photonic quasicrystal is made of alternating superconductors and dielectrics (SiO$_2$) with n$_L$ = 1.45. In particular, the superconductor is assumed to be YBa$_2$Cu$_3$O$_7$ with a critical high-Tc temperature (Tc = 93 K) and a London penetration depth at zero temperature $\lambda_L(0) = \lambda_0 = 145$ nm.

We adopt TMM approach to exhibit the transmittance, band gaps and characteristics of the hybrid GTM and GF photonic quasicrystals.

Figure 3 shows the transmittance spectrum, at normal incident angle for different n values.

We remark that the spectrum give a stacking of similar channels with zero transmission covering the whole frequency range. We also observe that the number of gaps increases with an increase of the lattice parameter n of GTM.

Also, sharp peaks of transmission appear for specific multiple frequencies. All peaks prohibit the stop band gaps and form a fine zone of propagation wave. This zone constitutes a little region of transmissions with small half bandwidth $\Delta f = 1.2$ THz. Similarly, the size of the output channels becomes narrow as n increases. Then, a large PBG zone was created. Thus, we note that the characteristics of channel filters are sensitive to lattice parameters of GTM sequence which organized the layers H and L. The similarity of transmission spectrum is caused by the self-similarity of geometrical GTM structures.

4.1.2 Effect of the thickness of superconductor on GTM structure

In this part, the superconductor's thickness is changed by varying the permittivity of its refractive index. **Figure 4** shows that a large PBG augments with an
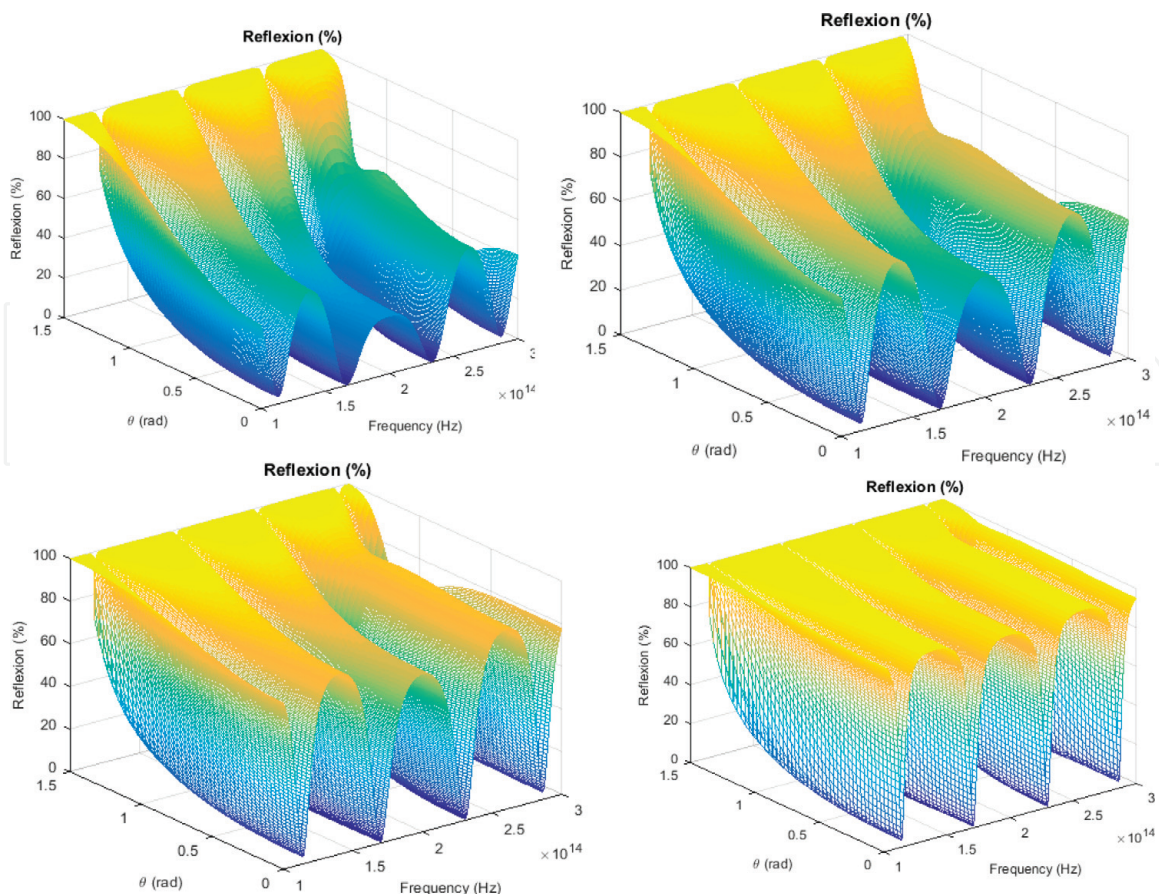

Figure 4.
The 3D reflectance spectrum through hybrid GTM(m, n) heterostructure at given values of superconductor's thicknesses: d$_s$ is set at 20, 40, 60 and 80 nm.

augmentation the thickness. Full gaps were obtained for d_s = 80 nm. The amplitude of oscillations around the channels with T = 0 decreases with an increase of d_s. Also, a set of peaks is obtained for high values of thickness. Accordingly, the dip of each gap increases when the thickness of $YBa_2Cu_3O_7$ increases, and the pseudo PBG becomes a gap with zero transmission. This improves the characteristics of channel filters.

4.1.3 Quality factor (Q)

In this part, we calculate the quality factor based on the following formula: $Q = \sim f_c / \Delta f$, where Δf is the Full Width at Half Maximum (FWHM) of transmission peak and f_c is the wavelength of maximum transmission.

Our calculation is summarized in **Figure 5** which gives the evolution of quality factor Q versus the frequency center of resonant transmission peak for different superconductor temperatures T. We remark that Q is very sensitive to the position of resonant peaks in 170–171 THz frequency range and it is inversely proportional to superconductor's temperature T. The FWHM are approximately equal for the lower frequencies and it sharply increase for the higher frequencies range. Then, a high pass filter can be obtained for lower T.

In order to show the consequences of the variation of parameter p of GTM sequence, we determine the transmittance T versus the frequency for p = 7.

As it can be seen from **Figure 6**, the number of defect modes or channels depends on the superconductor's thicknesses and the distribution of layers. Moreover, the transmission spectrum exhibit a stacking of narrow gaps without oscillatory behavior. The bandwidth of each gap decreases regularly for an increase of parameter n and it probably forms a great wide PBG covering all telecommunication frequency range. The number of the transmission peaks increases as p increases. The band gaps are symmetrical about the separated transmission due to the symmetry of layers within the GTM structure.

4.1.4 Effect of superconductor temperature on GTM structure

In this subsection, we study the influence of superconductor's temperature on transmission spectrum of 1D hybrid GTM structure for different incidence levels. Thus, we evaluate the characteristics of multichannel. Indeed,
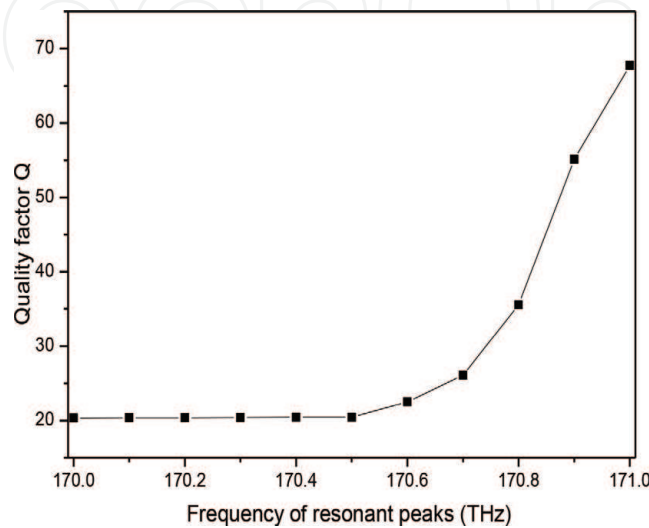

Figure 5.
Variation of factor quality Q of the GTM quasiperiodic multilayered stack containing a superconducting material versus frequency f (THz) at the frequency range between 170 and 171 THz.
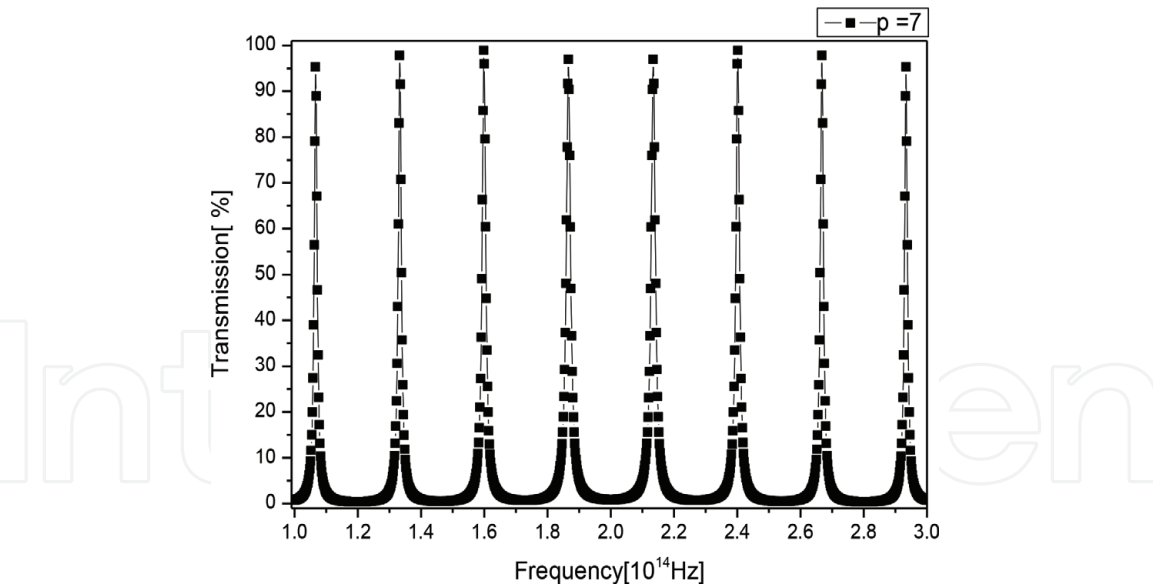
Figure 6.
A schematic view of transmittance spectra through the one dimensional photonic quasicrystals arranged according to GTM sequence for n = 2 and p = 7.
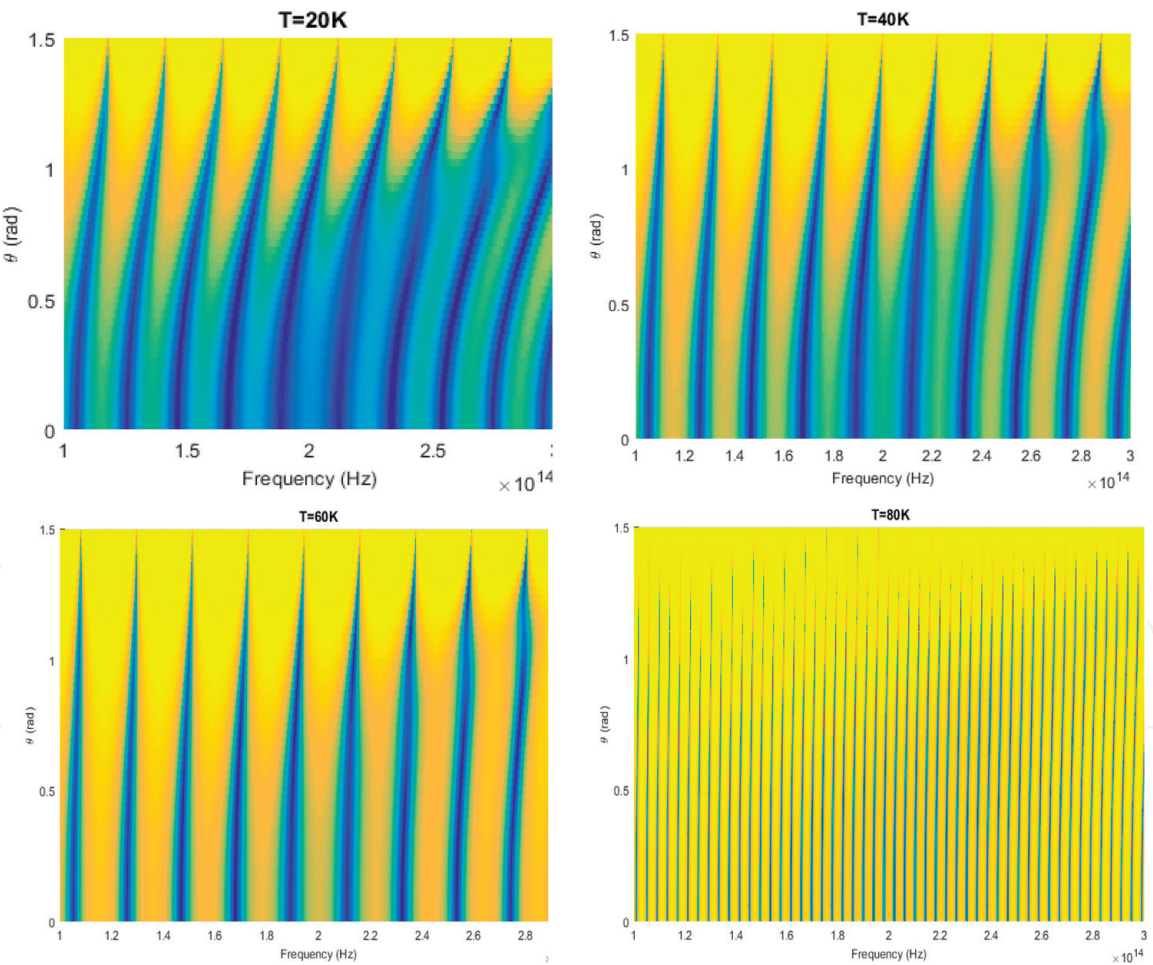

Figure 7.
A schematic view of distributed transmission of hybrid GTM photonic heterostructure versus frequency and incident angle for T = 20, 40, 60 and 80 K.

Figure 7 shows that GTM multilayer stack exhibits a specific zone with zero transmission (the yellow area) for different incident angles. In the corresponding band, the propagation wave is prohibited and reached the maximum recovers for θ = 1.5 rad.

Moreover, the spectrum presented a stack of band gaps and separated by sharp transmission peaks (the blue areas) allows the propagation of wave in this specific region of frequencies. The size of propagate zone within all PBG is sensitive to temperature T of $YBa_2Cu_3O_7$. The width of transmission peak within the channels increases progressively with the increase of T. A large zero of reflection bands is also noticed for T = 80 K, it covers all optical telecommunication frequency range and it constitutes perfect reflectors in these region.

4.1.5 Enhancement of PBGs by applying a particular deformation

In order to improve the characteristics of filtering channels, we apply a particular deformation h satisfying the following low $y = x^{h+1}$, where, x and y represent the coordinates of the main and the deformed GTM heterostructures, respectively.

We recall that in the main structure, two forms of layer, H and L are organized in a GTM sequence, where H and L are the superconductor and dielectric materials, respectively.

Then, the optical phase becomes: $\varphi_{j-1} = 2\pi/\lambda x_0' \cos\theta_{j-1}$. Here, the optical thickness after deformation noted x_0' satisfied the following form: $x_0' = \lambda_0/4\left(j^{th} - (j-1)^{th}\right)$. In this case, j and λ_0 indicate the optical thickness of jth layer which depends on deformation value h and the reference wavelength. According to this notion, **Figure 8** illustrates the distributed of H and L with low and high refractive indices of the main and deformed multilayered stack. We take h = 0.1 and m = n = 2.

Figure 9 shows the reflectance spectrum for a corresponding deformed GTM heterostructure. For the optimum value of deformation, similar peaks of transmission appear inside all PBGs. This selective channel of transmission is sensitive to parameter n of GTM. The reflection bands form a typical output multichannel. Also, the number of channels and transmission peaks within PBGs increase when n augments. The channel of each PBG becomes narrow as n increases. In this case, m was maintained fix at 2. As a result, the characteristics of PBG are improved by applying the deformation h. Consequently, it is possible to improve the filtering properties by varying the suitable configuration of GTM parameters and the deformation h.

In order to improve the characteristics of filtering channels, we apply a deformation to the whole thicknesses of the main GTM structure. **Figure 10** shows the distributed of transmission versus frequency for varying deformation h.
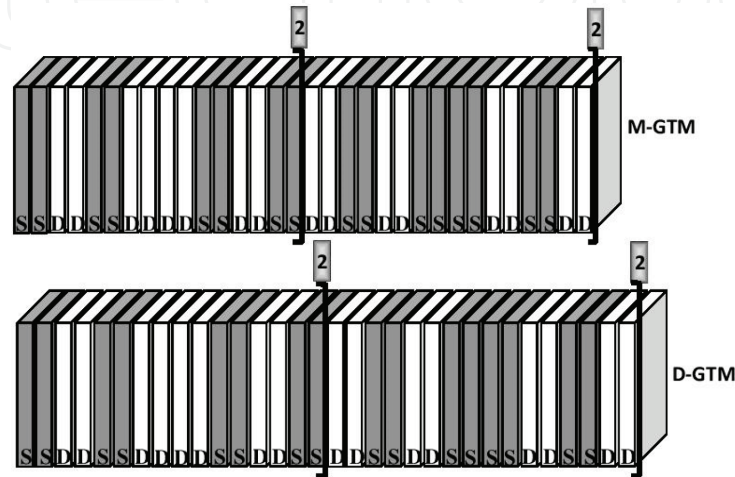

Figure 8.
Schematic representation of the main and deformed GTM photonic quasicrystals containing S and D materials, respectively. The deformation obeyed to the power law y = x^{h+1}.
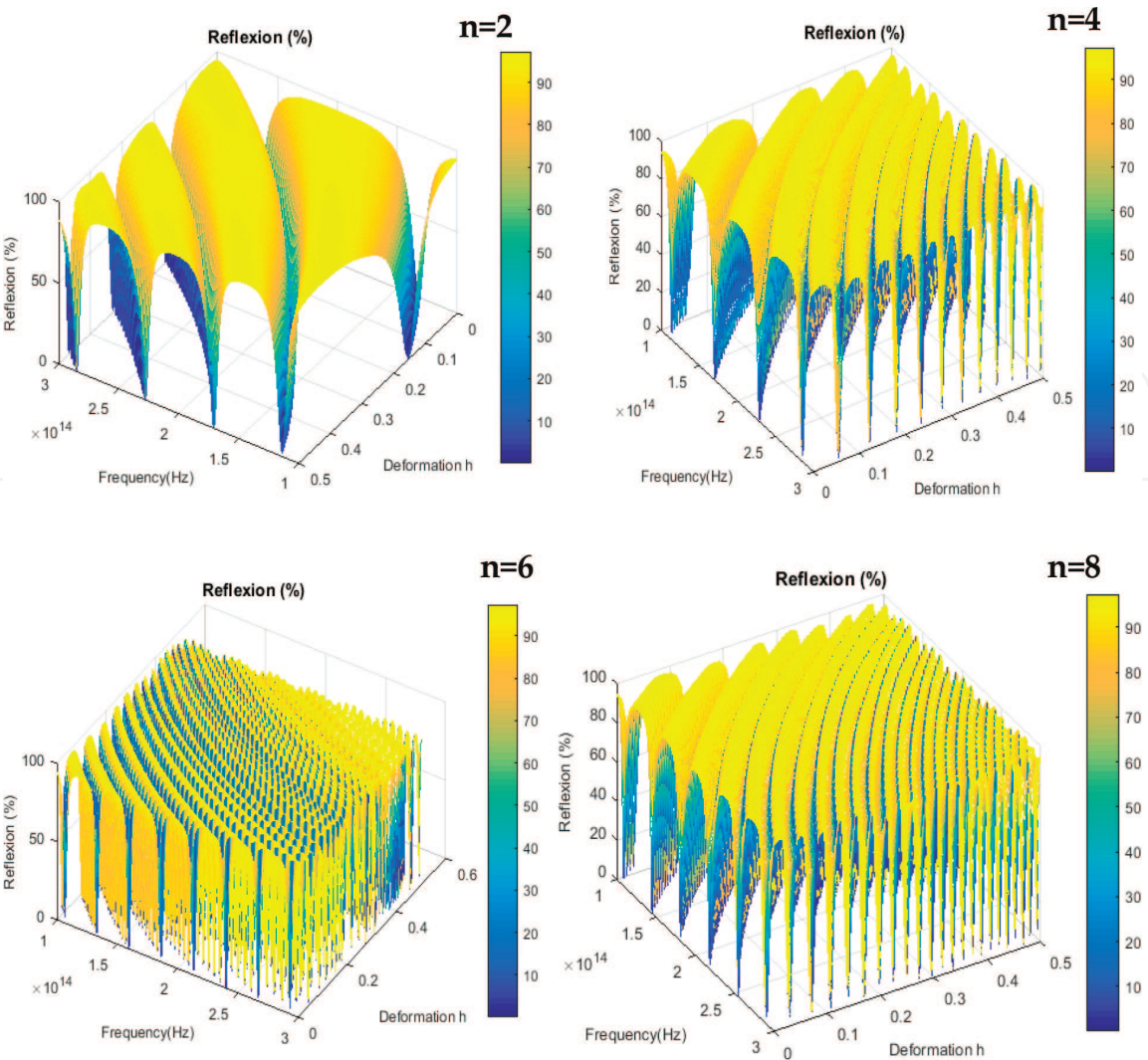
Figure 9.
3D reflectance spectrum at normal incidence from 1D GTM multilayered stack as a function of frequency (Hz) and deformation h with parameter n set to be 2, 4, 6, and 8.

The distribution of electric fields exhibits a stacking of a bending zone with zero transmission (yellow areas) and it is limited by harmonic peaks in blue fine zone. Then, these bending reflection bands are sensitive to superconductor's temperature. Thus, the PBGs are enhanced for an increase of T. In addition, the zone of transmission increases and the split peaks become narrow when T augments. Thus, the contrast indices of the two materials increases with T. Consequently, the considered factors cause broadening channels. Similarly, the intensity of transmission in all structures is reduced.

4.2 Generalized Fibonacci (GF) multichannel filters

4.2.1 The effect of GF(m, n) parameters

In this subsection, we study the properties of filtering through the 1D quasiperiodic GF multilayered stacks which contain superconducting materials. The considered common sequence suggests a typical aperiodic distribution of two alternating layers H and L with high and lower refractive indices, respectively.

The two constituent materials are arranged following the GF(m, n) sequence for m = pn, where p is a positive integer. We found that the transmission spectrum give similar band gaps which depend on the distributed layers initially fixed by the GF parameters (**Figure 11**). Therefore, the channel with zero transmission becomes
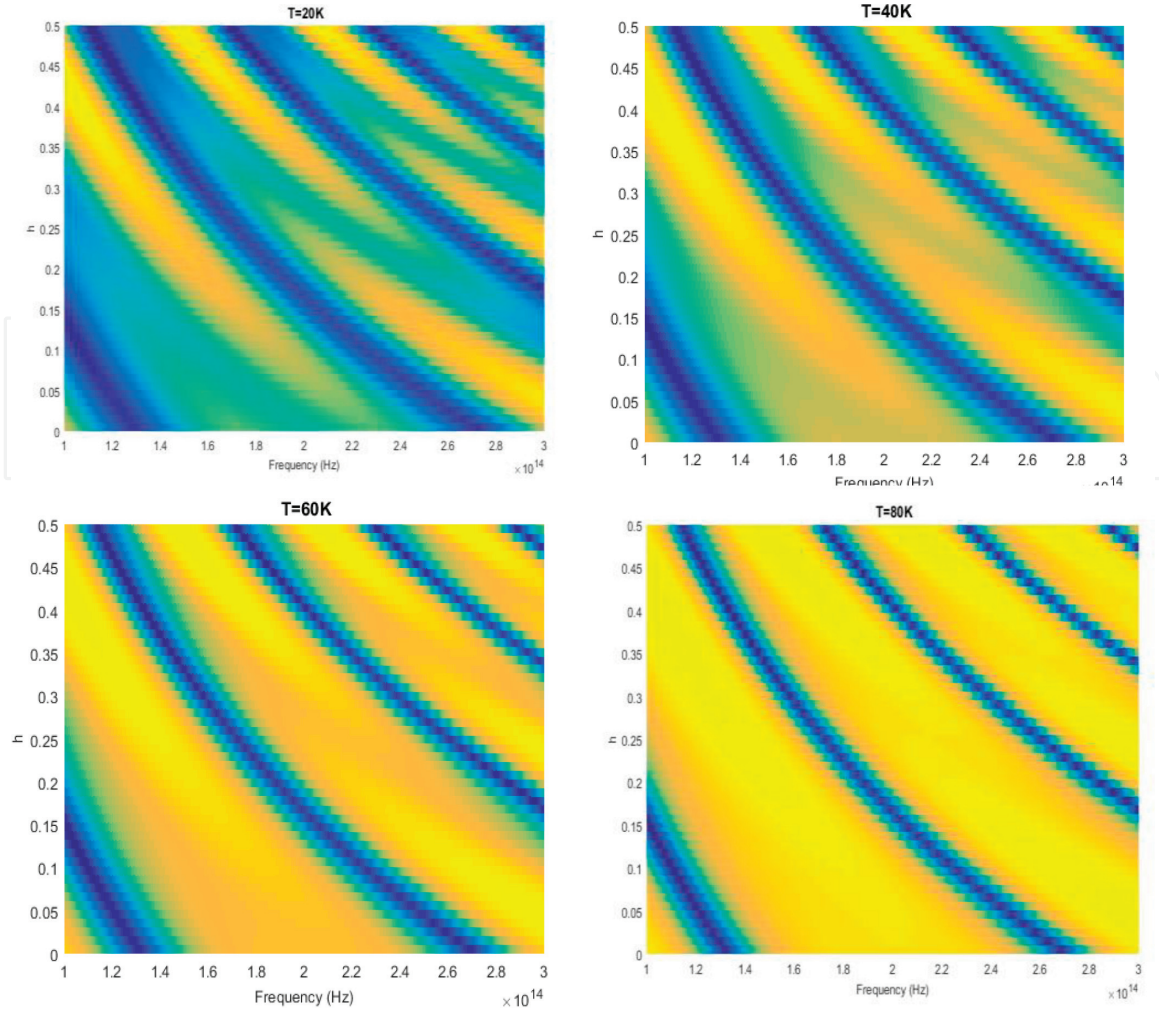
Figure 10.
A schematic view of distributed transmission of hybrid GTM multilayer stacks as a function of deformation degree h and frequency for different temperature values.

narrow when p increases. The hybrid GF heterostructure possess an oscillation transmission around all PBGs. Moreover, the stacking channels are symmetric around the reference frequency.

4.2.2 The effect of contrast indices on hybrid GF(m, n) system

In this subsection, we show the effect of the contrast indices between two alternating materials on the filtering properties. The contrast indices satisfy the following relation: $\Delta n = n_s - n_d$ with n_s and n_d represent the refractive indices of superconductor and dielectric, respectively. The same conditions are conserved to extract the transmission through the considered GF heterostructure.

Figure 12 gives the transmittance spectrum for different values of contract indices. We mention that the GF form exhibits a large frequency range with zero transmission and shows at limited gap a sharp transition from 0 to 1 at given Δn.

The intermediate point between inhibited and propagated waves indicates the cut-off frequency that allows the signal to propagate again, showing itself as a stop band filer. Moreover, we remark that the positions of the two cut-off frequencies f_{cL} and f_{cH} are very sensitive to the contrast indices. As long as Δn augments, the PBG increases similarly with the high cut-off frequency. Such interesting property may be applied to design a perfect reflector for high refractive index of superconductors. Thus, this type of reflectors exhibits a large bandwidth that contains the optical telecommunication frequency range.
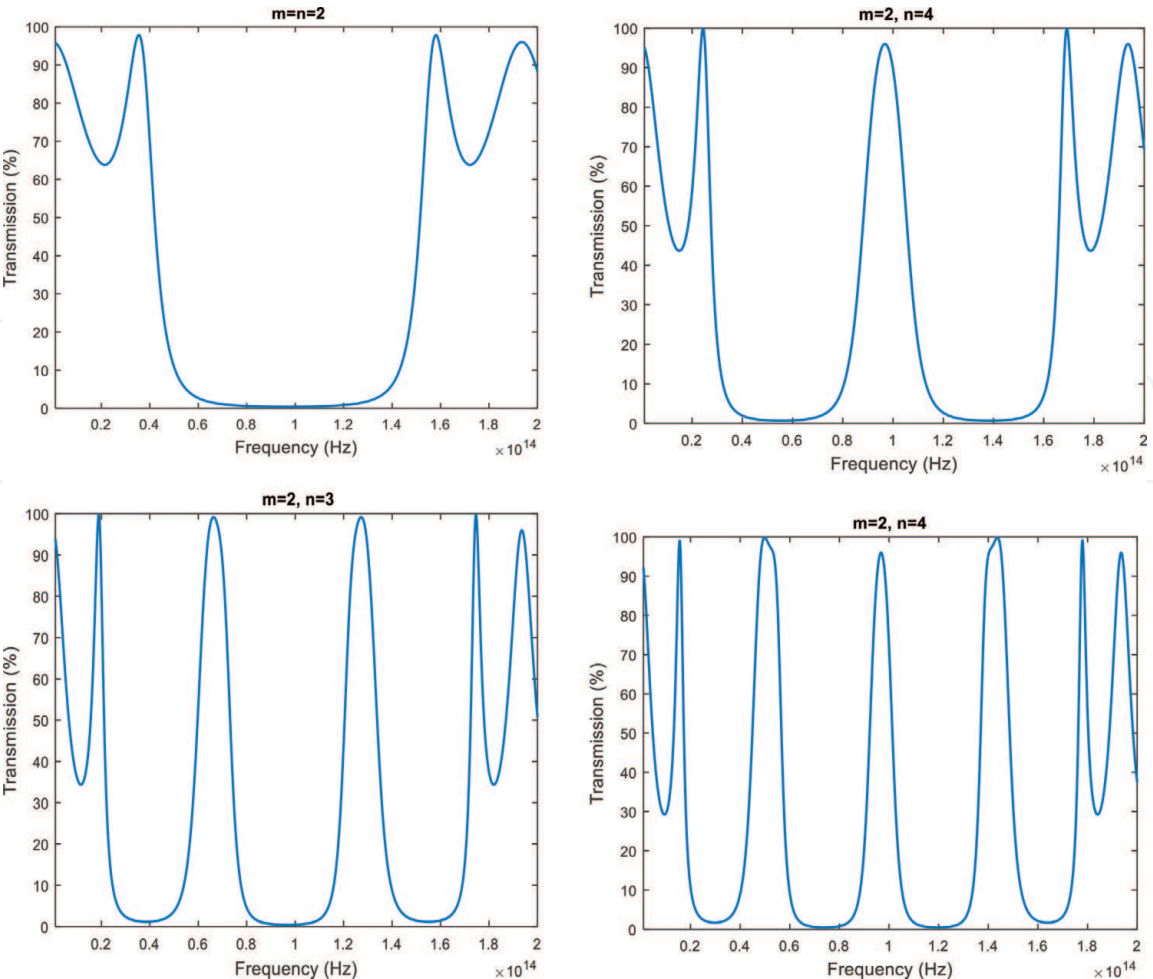
Figure 11.
Transmittance spectrums from 1D hybrid GF structure containing alternating dielectric/superconducting layers at given parameters: n set to be 2, 3 and 4 with m = 2.
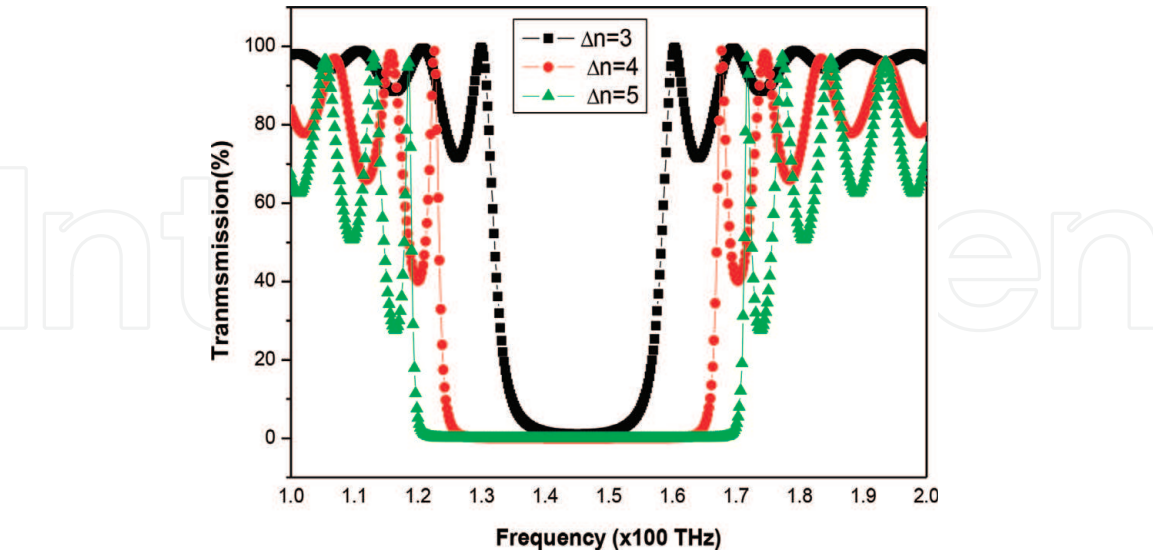

Figure 12.
Schematic representation of transmittance spectrums from 1D GF multilayered stacks at given Δn: n set to be 3,4 and 5 with n_d = 1.45.

5. Conclusion

The filtering properties of the 1D hybrid heterostructure built according to the GTM and GF sequences are investigated in this study. It was observed that the two common quasiperiodic sequences exhibits a multitude of channels with zero

transmission for specific values of parameters m and n. In particular, the spectrum of GTM system possesses similar narrow gaps without oscillation beams at a given parameter: m = 2 pm. Indeed, a sharp transmission peak is appreciated in the whole frequency range whose positions are sensitive to superconductor temperature. Therefore, the considered system can be useful as a selective pass band multichannel filter whose narrow bandwidth can be adjusted by temperature. In addition, the main GTM system gives staking gaps which are enhanced by applying a specific deformation. Similarly, the GF heterostructure suggests an identical channel frequencies without transmission as compared to GTM system but their spectrum have particular oscillations around the cut-off frequency. Thus, the properties of filtering change by modifying the type of sequences and the parameters of constituent materials.

Author details

Youssef Trabelsi[1,2]

1 Photovoltaic and Semiconductor Materials Laboratory, El-Manar University-ENIT, Tunis, Tunisia

2 Department of Physics, King Khalid University, Abha, KSA

*Address all correspondence to: yousseff.trabelsi@gmail.com

IntechOpen

References

[1] Zamani M. Spectral properties of all superconducting photonic crystals comprising pair of high-high, low-low or high-low temperature superconductors. Physica C: Superconductivity and Its Applications. 2016;**520**:42-46

[2] Srivastava SK. Study of defect modes in 1d photonic crystal structure containing high and low Tc superconductor as a defect layer. Journal of Superconductivity and Novel Magnetism. 2014;**27**:101-114

[3] Upadhyay M, Awasthi SK, Shiveshwari L, Srivastava PK, Ojha SP. Thermally tunable photonic filter for WDM networks using 1D superconductor dielectric photonic crystals. Journal of Superconductivity and Novel Magnetism. 2015;**28**: 2275-2280

[4] Rahimi H. Analysis of photonic spectra in Thue-Morse, double-period and Rudin-Shapiro quasiregular structures made of high temperature superconductors in visible range. Optical Materials. 2016;**57**:264-271

[5] Zhang HF, Liu SB, Yang H. Omnidirectional photonic band gap in one dimensional ternary superconductor-dielectric photonic crystals based on a new Thue Morse aperiodic structure. Journal of Superconductivity and Novel Magnetism. 2014;**27**:41-52

[6] Roshan Entezar S. Photonic crystal wedge as a tunable multichannel filter. Superlattices and Microstructures. 2015;**82**:33-39

[7] Lin WH, Wu CJ, Yang TJ, Chang SJ. Terahertz multichannel filter in a superconducting photonic crystal. Optics Express. 2010;**18**:27155-27166

[8] Zhang HF, Liu SB, Kong XK, Bian BR, Ma B. Enhancement of omnidirectional photonic bandgaps in one-dimensional superconductor dielectric photonic crystals with a staggered structure. Journal of Superconductivity and Novel Magnetism. 2013;**26**:77-85

[9] Barvestani J. Omnidirectional narrow bandpass filters based on one-dimensional superconductor dielectric photonic crystal heterostructures. Physica B. 2015;**457**:218-224

[10] Liu JW, Chang TW, Wu CJ. Filtering properties of photonic crystal dual-channel tunable filter containing superconducting defects. Journal of Superconductivity and Novel Magnetism. 2014;**27**:67-72

[11] Taherzadeh S, Vafafard A, Maleki MA, Mahmoudi M. Total reflection and transparent window in one-dimensional duplicated superconducting photonic crystal. Journal of Superconductivity and Novel Magnetism. 2013;**26**: 2911-2917

[12] Aly AH. Metallic and superconducting photonic crystal. Journal of Superconductivity and Novel Magnetism. 2008;**21**:421-425

[13] Tinkhman M. Introduction to Superconductivity. 2nd ed. New York: McGraw-Hill; 1996

[14] Mourachkine A. Room-Temperature Superconductivity. 1st ed. United Kingdom: Cambridge International Science Publishing; 2004

[15] Soltani O, Zaghdoudi J, Kanzari M. Analysis of transmittance properties in 1D hybrid dielectric photonic crystal containing, superconducting thin films. Physica B: Physics of Condensed Matter. 2018;**538**:62-69

[16] Moretti L, Rea I, Rotiroti L, Rendina I, Abbate G, Marino A, et al. Photonic band gaps analysis of Thue-Morse multilayers made of porous silicon. Optics Express. 2006;**14**:6264-6272

[17] Rostami A. Generalized Fibonacci quasiphotonic crystals and generation of superimposed Bragg Gratings for optical communication. Microelectronics Journal. 2006;**37**:897-903